Ritter, O., Haak, V., Rath, V., Stein, E., Stiller, M. (1999): Very high electrical conductivity beneath the Münchberg Gneiss area in Southern Germany: implications for horizontal transport along shear planes. - Geophysical Journal International, 139, pp. 161—170.

DOI: http://doi.org/10.1046/j.1365-246X.1999.00937.x

Geophys. J. Int. (1999) **139,** 161–170

Very high electrical conductivity beneath the Münchberg Gneiss area in Southern Germany: implications for horizontal transport along shear planes

Oliver Ritter,[1] Volker Haak,[1] Volker Rath,[2] Eckardt Stein[3] and Manfred Stiller[1]

[1] *GeoForschungsZentrum, Telegrafenberg,* D-14473 *Potsdam, Germany. E-mail:oritter@gfz-potsdam.de.*
[2] *Technische Universität Berlin, Institut für Angewandte Geophysik, Petrologie und Lagerstättenkunde, Ackerstrasse* 71–76, D-13355 *Berlin, Germany*
[3] *Institut für Mineralogie, Technische Universität Darmstadt, Schnittspahnstrasse* 9, D-64287 *Darmstadt, Germany*

Accepted 1999 May 28. Received 1999 May 28; in original form 1998 August 13

SUMMARY

New magnetotelluric data from the Münchberg Gneiss complex in Southern Germany reveal a zone of extremely high electrical conductivity. 1-D modelling of the data is justified in the period range 0.01 to 10 s. At least three layers are required to explain the steepness of the apparent resistivity curves, and the best-fitting models comprise four layers with successively higher conductivities. The layers of highest conductivity at depths between 2.2 and 3.6 km correlate with pronounced bands of high seismic reflectivity (profile DEKORP 85-4N). The Münchberg complex is today widely recognized as a tectonic klippe, consisting of rocks whose metamorphic and stratigraphic order is inverted rather than overturned. The material was transported into its present position by predominantly horizontal tectonic forces along shear zones. We interpret the high conductivity and high reflectivity as remnants of this transport process.

Key words: DEKORP85-4N, electrical conductivity, magnetotellurics, Münchberg Gneiss complex, shear zones, Variscan orogeny.

INTRODUCTION

Crystalline nappes play an important role in the reconstruction of fossil tectonic processes of the basement. Nappes are characterized as allochthonous rock assemblages that have been transported laterally by tectonic processes. The distance over which the rocks are transported can reach hundreds of kilometres. The Münchberg Massif (MüMa) in Southern Germany is such a nappe; it consists of an assemblage of gneissic rocks, which were transported to their present location in NE Bavaria during the Variscan orogeny (Franke 1980). The tectonic interpretation of this gneiss complex, however, has been disputed among geologists for more than 100 years, and there have been problems in deciding how and which geophysical methods should be deployed to support the interpretations.

Renewed interest in the area arose within the framework of recent research of the Mid-European Variscan Belt (e.g. DEKORP & Orogenic Processes Research Groups 1998; Schäfer 1997; Franke *et al.* 1995; Behr & DEKORP Research Group (B) 1994; Weber & Behr 1983). In order to understand the regional geology, it is essential to decide how the MüMa deep crustal, high grade rocks (the highest grade metamorphic facies comprise eclogite, which is created under *PT* conditions of the Earth's mantle) arrived at their present position.

The interpretation of the MüMa formations also played a major role in the choice of the final location for the German deep drilling project KTB, which is located 80 km further southeast. In this context, and also as part of the German DEKORP programme, the MüMa was investigated with reflection seismics and numerous other geophysical methods. In 1981, audiomagnetotelluric (AMT) measurements were carried out at 20 locations across the MüMa (Haak *et al.* 1985). At that time, AMT instruments that could record data at high frequencies (1000–1 Hz) were just becoming technically feasible; however, a wide variety of electromagnetic noise sources, combined with high surface resistivities, prevented an accurate assessment of the data quality. Although the noise problem has worsened over the last 15 years, there have been considerable improvements in geophysical instrumentation and data processing tools (Egbert & Booker 1986; Larsen *et al.* 1996; Egbert 1997; Ritter *et al.* 1998). These developments provided the impetus to re-investigate the MüMa with modern equipment.

A large number of electrical conductivity anomalies have been detected in the Earth's crust around the world. There is no clear consensus as to the causes and origins of these anomalies, particularly in crystalline regimes. However, in the light of the 9.1 km deep KTB drill hole, we now have evidence that high electrical conductivity can be linked with shearing processes. At the KTB site, zones of high electrical conductivity

have been found to be connected with fractured sections of the crust, while the 'wet' but intact crust is very resistive (ELEKTB 1997).

GEOLOGICAL BACKGROUND

The Münchberg Massif represents an exotic klippe as part of a former widespread, continuous nappe complex which has been preserved from erosion by its protected position in the Vogtland syncline. It consists of four low to high grade metamorphic thrust sheets, overlying an allochthoneous, weakly metamorphosed metasedimentary unit which itself can be separated into three thrust sheets. The tectonometamorphic units from top to bottom are (see Fig. 1): Hangend series, Liegend series, Randamphibolite series and Phyllit-Prasinit series.

The Hangend series shows a variegated lithology, comprising hornblende gneisses, amphibolites and paragneisses with interlayers of calcsilicate rocks and marbles. At the base, bodies of serpentinite, eclogite and eclogite-amphibolite with diameters from tens of metres to several kilometres are abundant. The metamorphic peak conditions are displayed by the eclogites, with $P_{max} > 2.5$ GPa and $T_{max} \sim 650\,^{\circ}$C, whereas the metamorphic imprint of gneisses of the Hangend series show only amphibolite facies conditions, with pressures of about 1.2 GPa and related temperatures of $\sim 650 \pm 30\,^{\circ}$C (O'Brien 1996). The age of the high-pressure metamorphism is still under discussion,

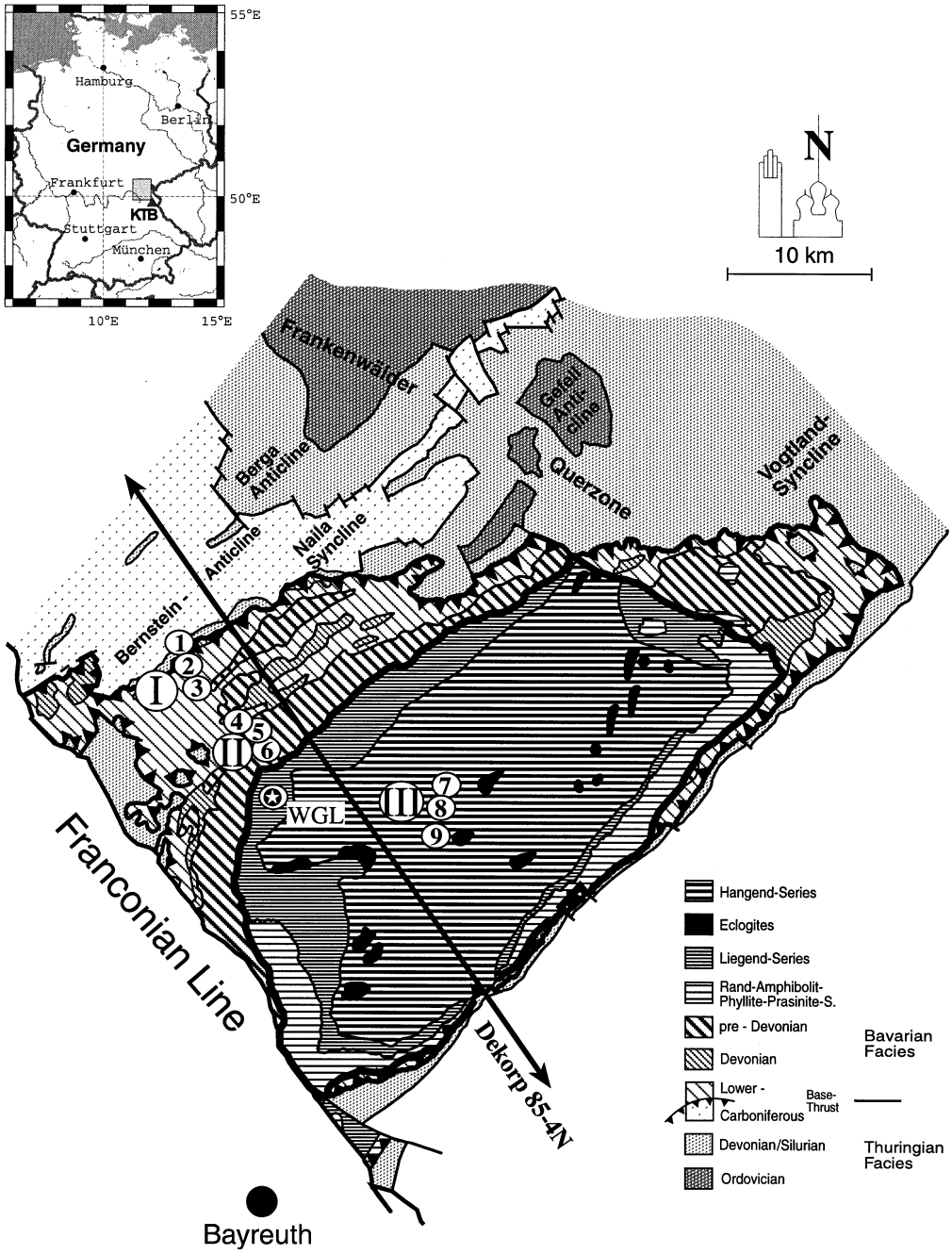

Figure 1. Location map of the MT sites and simplified geological map of the Münchberg Massif. Each station array (labelled I–III) consists of three AMT sites (labelled 1–9). Site WGL was measured in a previous survey (see text).

but the latest published data (Sm/Nd, whole rock–pyroxene–garnet core) from Stosch & Lugmair (1990) show an isochrone age of 395 ± 4 Ma.

Compared with the Hangend series, the Liegend series shows a monotonous lithology, consisting of paragneisses, which are intercalated with an orthogneiss sheet and a few lenses of metagabbros. The peak-metamorphic conditions, of $P \sim 1.2$ GPa and $T \sim 650\,^{\circ}$C determined at a metagabbro, are similar to the amphibolite facies conditions of the Hangend series; no evidence for high-pressure metamorphism has been identified in these rocks so far (O'Brien 1996). According to Müller-Sohnius *et al.* (1987), both units were spatially separated until about 385 Ma, with a common subsequent cooling history starting at about 380 Ma (K/Ar, Ar/Ar: hornblende and muscovite).

The Randamphibolite series is built up solely by amphibolites, which may be massive, banded or schistose. Their mineral assemblages point to lower amphibolite facies metamorphic conditions. A characteristic feature is the intense mylonitization at the tectonic contacts to the over-and underlying units.

The Prasinit-Phyllite series consists of an alternation of basic to intermediate lavas and pyroclastics with silty shales which are metamorphosed under greenschist facies conditions and which is overprinted by brittle deformation at the contact to the underlying nappe. Microfossils in the phyllites indicate a Proterozoic protolith age (Pflug & Reitz 1987).

Mineral lineations and mineral-stretching lineations in mylonites and ductile shear zones as well as other kinematic markers indicate an accretion of the metamorphic nappes in an east–west direction with transport towards the west.

The underlying, unmetamorphosed to anchimetamorphic tectonic units from top to bottom are the Randschiefer series, with a lithology similar to the Prasinit-Phyllite series but Ordovician in age (fossil dated), Silurian and Devonian cherts, and lower Carboniferous flysch sediments. All these allochthoneous metasedimentary thrust sheets belong to the Bavarian facies, which is overthrusted onto the autochthoneous sediments of the Thuringian facies at the basal thrust, and each of these units is separated from the others by tectonic contacts.

Brittle deformations with NW–SE-orientated slickensides on the thrust planes, including the basal thrust, clearly point to a NW–SE-directed accretion of the metasedimentary thrust sheets with a final, NW-directed emplacement of the entire nappe unit in a superficial, shallow environment.

Summarizing the geological constraints, the Münchberg nappe pile consists of two tectonic thrust sheet units:

(1) A metamorphic one, which clearly shows a medium- to high-pressure metamorphic imprint with an inverse zonation of the baric isograde and an accretion and transport toward the west.

(2) A (meta-)sedimentary thrust sheet complex, with an inverse, but not overturned, stratigraphic sequence typical for thrust sheets, with an accretion and final emplacement toward the northwest.

MAGNETOTELLURIC AND SEISMIC DATA

Both the GeoForschungsZentrum Potsdam and the Technische Universität Berlin use a new generation of instruments called SPAM (short-period automatic magnetotellurics) MkIII, developed at the University of Edinburgh (Dawes 1990). SPAM MkIII operates as a networked instrument in such a way that compatible parts of the system can be interconnected in many different ways. The information from neighbouring sites can be used in data processing schemes to reduce the influence of noise. For the data analysis we applied a method which uses the coherency and expected uniformity of the magnetic source field as quality criteria (Ritter *et al.* 1998). Data are rejected (i) if the horizontal magnetic field components at two given sites have a low coherence (coherency criterion) or (ii) if the response functions are considerably different from unity (target criterion). Time segments with inconsistent horizontal magnetic field data are thereby removed, leaving a reduced but cleaned data set for the estimation of robust, remote referenced, magnetotelluric response functions.

Overall, we recorded at three station arrays, each consisting of three sites. The station arrays are labelled I to III in Fig. 1; the approximate distances between arrays I and II, and II and III are 4 and 8 km, respectively. Array III was located at the centre of the gneiss complex, near the town of Münchberg, while arrays I and II were installed close to the boundary to the Carboniferous sediments of the Bavarian facies. The site locations are summarized in Table 1.

Fig. 2 shows the results from sites I/3, II/6 and III/9 as apparent resistivity and phase curves, calculated from orthogonal components of the electric and magnetic fields in a geographical coordinate system. In this convention, the *XY*-polarization curves in Fig. 2 correspond to an electric field measured in a NS direction, and the *YX*-polarization to an electric field measured in an EW direction. The data of site II/6 are extended with long-period results (100–10 000 s) from site WGL (see Fig. 1), which were recorded in 1992 by the Free University of Berlin (Gürtler & Schuarz 1994; Börner 1995). It is worth mentioning that the data from the two sites coincide and overlap, in spite of the fact that sensors, loggers, processing and personnel were all different. All apparent resistivity and phase curves show very similar patterns. The apparent resistivity curves decrease over more than three decades at an angle of almost 45°, while the phases are consistently above 45°, reaching values of up to 85°. Diverging apparent resistivity and phase curves for the long-period data of site WGL in Fig. 2 indicate more complicated structures as the induction range widens. Induction arrows, as indicators for lateral conductivity variations, are relatively small (<0.25) in the relevant period range between 0.01 and 10 s. However, the reversed orientation of the real induction arrows, as plotted at a frequency of 5.7 Hz in Fig. 3, hint at a zone of higher conductivity between station arrays I and III.

Table 1. Locations of the magnetotelluric sites, as plotted in Fig. 1.

Site No	Gauß-Krüger Easting	Northing	Geographic Longitude	Latitude
I/1	4466.5500	5570.6250	E11°31′31.06″	N50°16′18.24″
I/2	4466.7750	5570.1750	E11°31′43,76″	N50°16′03.65″
I/3	4467.2150	5569.4500	E11°32′06.47″	N50°15′39.73″
II/4	4470.1375	5566.7125	E11°34′56.47″	N50°14′12.16″
II/5	4470.6625	5566.2875	E11°35′27.53″	N50°14′02.03″
II/6	4470.7500	5565.9375	E11°35′31.76″	N50°13′47.03″
III/7	4481.4125	5561.5000	E11°44′22.86″	N50°11′28.39″
III/8	4481.4250	5560.9250	E11°44′23.49″	N50°11′06.08″
III/9	4481.1000	5560.1875	E11°44′07.62″	N50°10′43.38″

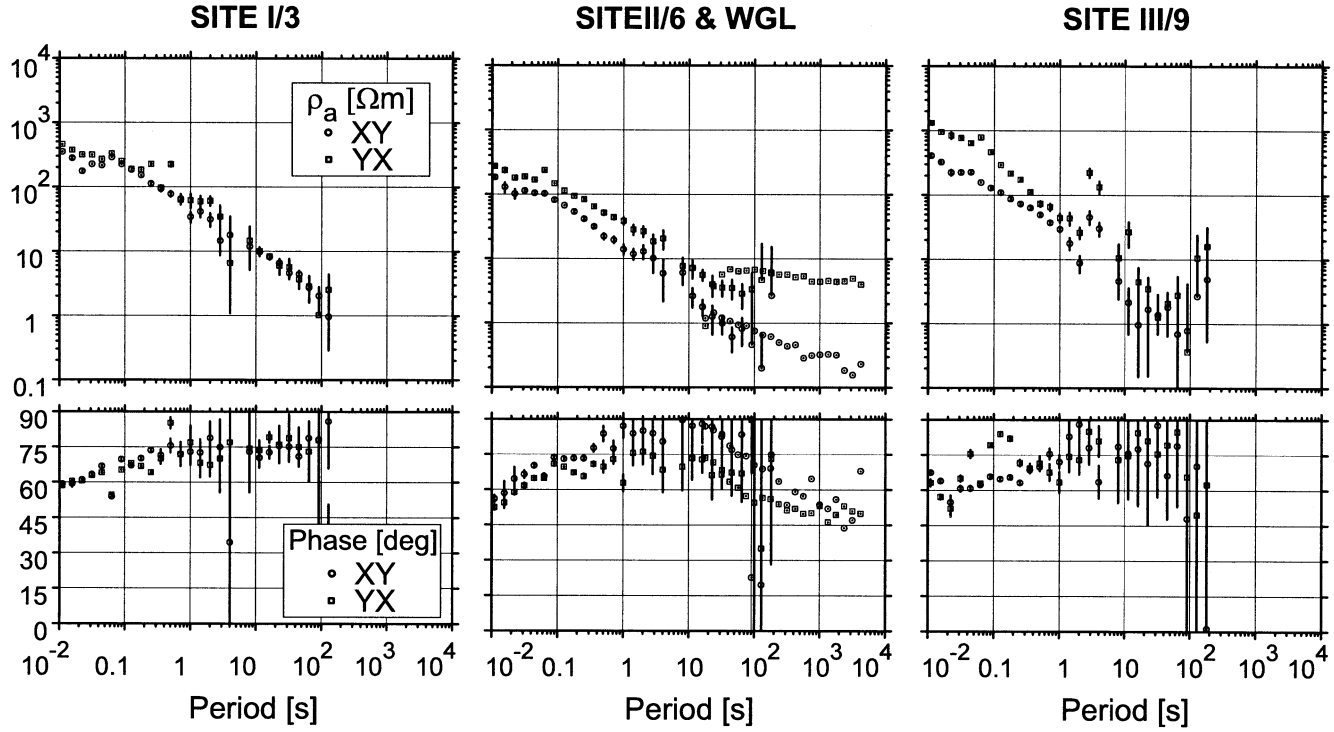

Figure 2. *XY*- (circles) and *YX*- (squares) polarizations of the apparent resistivity (ρ_a) and phase (Φ) curves. Each station array is represented by one site. Site II/6 is extended with long-period data from site WGL. Steeply decreasing ρ_a curves indicate a high electrical conductivity anomaly at depth.

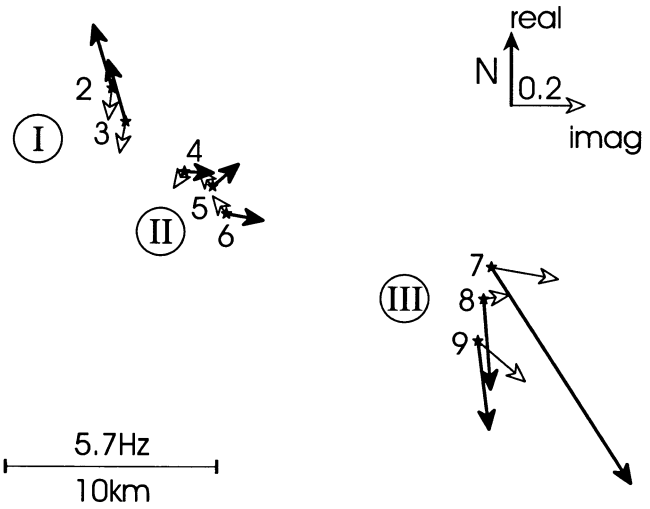

Figure 3. Real and imaginary induction arrows plotted at a frequency of 5.7 Hz. In Wiese convention the arrows tend to point away from the conductive side of a nearby conductivity contrast. See Fig. 1 for comparison with surface geology.

Fig. 4(a) shows the result of a 2-D Occam inversion (DeGroot-Hedlin & Constable 1990). The model responses and measured data from seven sites–sites I/1 and III/7 could not be used—are given in Fig. 4(b). For the inversion, the impedance tensor and vertical magnetic field transfer function data are rotated by $-60°$, as the sites align along a profile striking S60°E (compare with Fig. 1). Because of the irregular site distribution and large error bars in some frequency bands, this data set is not really suitable for a 2-D inversion. While the model should therefore not be over-interpreted, it is useful to discuss some of the main features of the data in Fig. 4(a): (1) the upper crust is resistive (100–1000 Ω m) beneath station arrays I, II and III; (2) the entire lower crust becomes very conductive ($\leq$1 Ω m) from depths of between 2.5 and 3.5 km; and (3) between station arrays II and III a conductive zone reaches the surface. This zone is probably most clearly expressed in the data by the reversed vertical magnetic field response functions between arrays II and III. The model responses shown in Fig. 4(b) are the results of an inversion which seeks to fit all data—the vertical magnetic field responses, TE, and TM mode—without static shift correction. The initial model for each inversion was a 100 Ω m homogeneous half-space.

The unconstrained 2-D Occam inversion generates a model showing resistivities of 1 Ω m for the entire lower crust and upper mantle (to a depth of 300 km!), which is not geologically plausible. A comparison of Figs 2 and 4(b) shows that the apparent resistivity and phase curves are similar at all sites, for both the rotated and unrotated data sets. The fact that the *XY*- and *YX*-polarizations of apparent resistivity and phase curves are approximately parallel at all sites also indicates a predominantly 1-D character of the subsurface. This observation is supported further by qualitative measures, such as small skew values and undetermined rotation angles for both conventional tensor analysis (Swift criterion) and tensor decomposition methods (Bahr 1988; Groom & Bailey 1989). To discuss alternative conductivity models we resort therefore to 1-D modelling procedures.

A wide variety of tools for forward and inversion calculations is available for 1-D modelling of magnetotelluric data. However, each has its own philosophy for deciding how much structure (i.e. number of layers and their thickness) is necessary

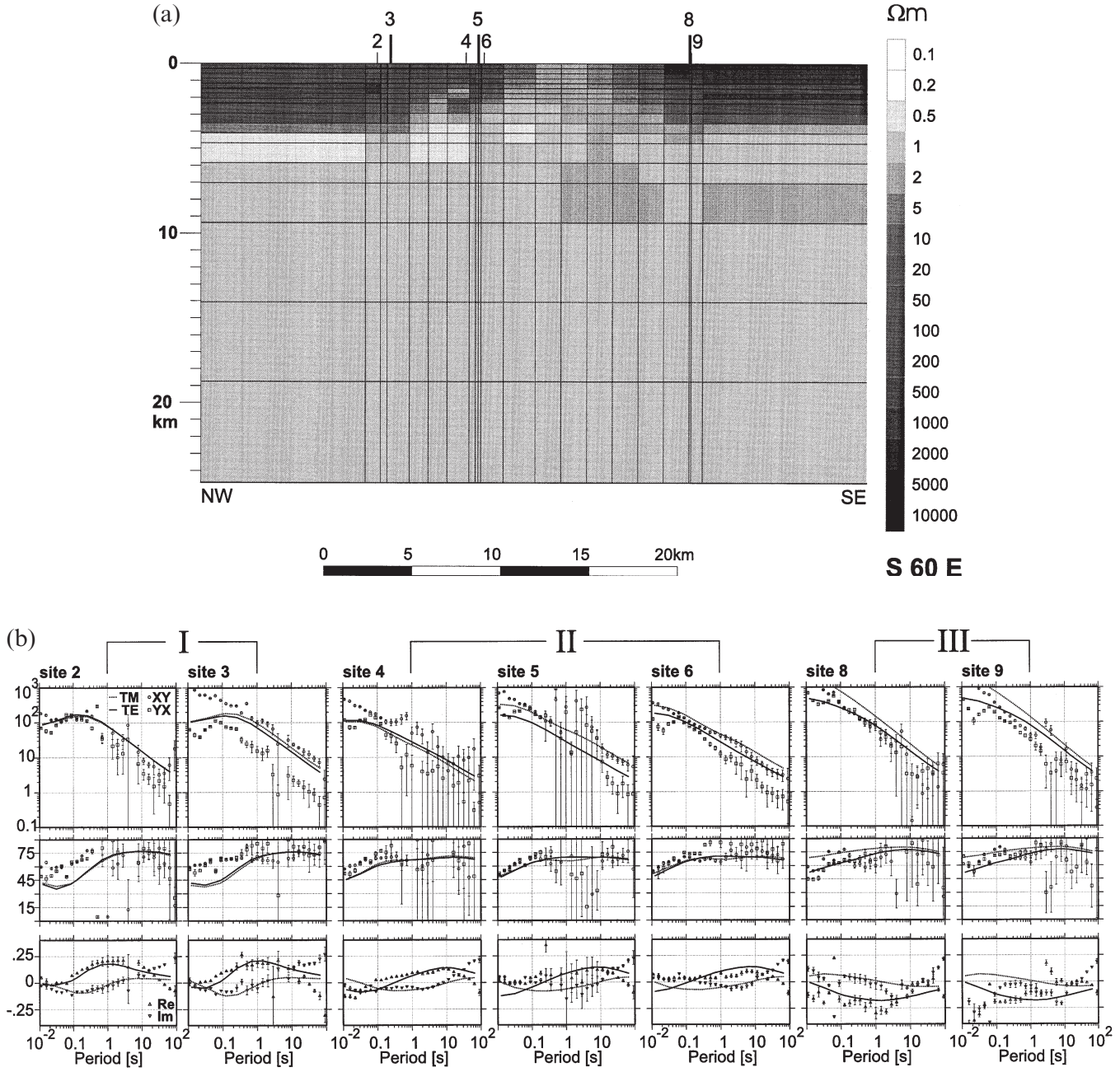

Figure 4. (a) Result of a 2-D Occam inversion of seven sites: the regularization grid is 74 × 31 nodes. Dark shaded areas indicate resistive blocks; light greys indicate conductive cells. The model shows resistivities of 1 Ω m for the entire lower crust and upper mantle. (b) Comparison of model responses (lines) with field data (symbols). The field data are rotated by −60°. The panels show apparent resistivity at the top, phase in the middle, and vertical magnetic field response functions at the bottom.

to understand the subsurface reality or sufficient to explain a certain data set. Most of our model calculations in this paper are based on a standard Marquardt–Levenberg least-squares fitting method which is part of the GEOTOOLS data interpretation package (Geotools 1997). To fit the data we calculate apparent resistivity and phase curves from rotationally invariant, averaged impedances: $Z_{avg} = (Z_{xy} - Z_{yx})/2$.

Fig. 5 demonstrates that a simple two-layer model of a resistor over a conducting half-space is not suitable to fit the data. The diagram shows 1-D responses of five different two-layer models. The top layer has a fixed resistivity of 256 Ω m, while the resistivities of the second, more conductive layer vary between 128 and 0.25 Ω m. On the right-hand side of Fig. 5 the model responses are plotted together with the averaged apparent resistivity and phase curves of site II/6. Model 3, with a resistivity ratio of 1 : 32, can partially explain the data but a more conductive second layer worsens the fit. While a model with at least three layers is required to represent the data, we observe consistently smaller misfits with four-layer models. Fig. 6 compares four-layer 1-D inversion responses with the measured data of sites I/3, II/6 and III/9; the modelling results are shown in Fig. 8 and Table 2. Obviously, the models suggest continuously increasing conductivity with depth at all sites.

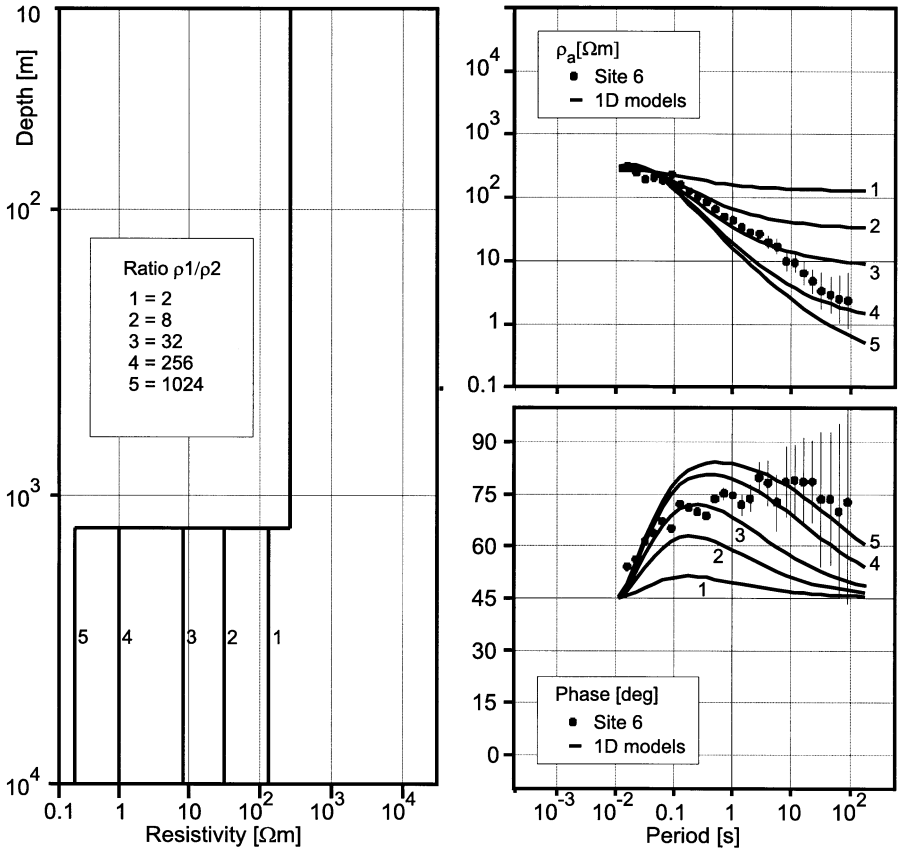

Figure 5. The slope of the steeply decreasing apparent resistivity curves cannot be explained by simple two-layer models composed of a resistive top over a conductive half-space. At least three layers are required to fit the data.

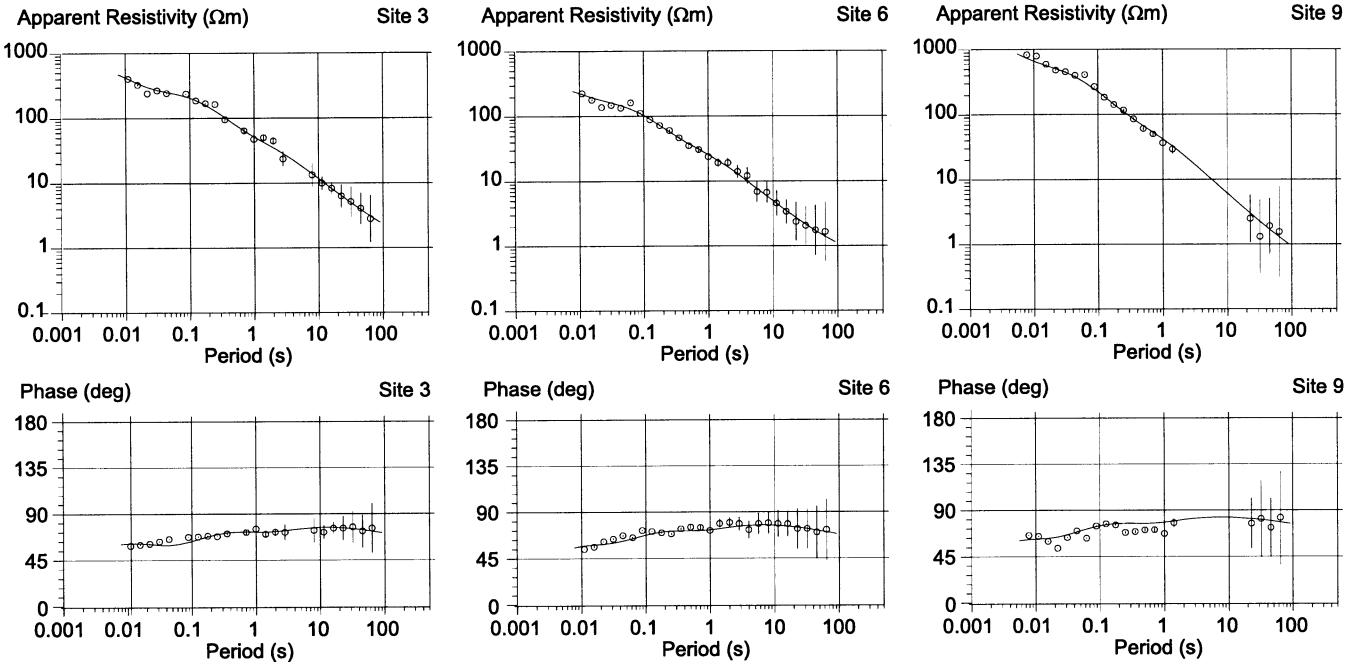

Figure 6. Rotationally invariant, averaged apparent resistivity and phase curves (circles), together with the responses of the best-fitting four-layer 1-D models (solid line). The conductivity models are plotted in combination with the seismic reflection data in Fig. 8.

Table 2. Summary of four-layer 1-D Marquardt–Levenberg inversion results. Depth values specify the distances to the top of the layers.

Site I/3 Resistivity [Ω m]	Depth [m]	Site II/6 Resistivity [Ω m]	Depth [m]	Site III/9 Resistivity [Ω m]	Depth [m]
634	0	261	0	1017	0
97	590	50	514	118	759
4.8	2043	3.7	1245	2.8	1701
0.26	3751	0.27	2215	0.16	2458
rms ($\ln \rho_a$)	rms (Φ)	rms ($\ln \rho_a$)	rms (Φ)	rms ($\ln \rho_a$)	rms (Φ)
4.59	9.52	2.88	3.33	6.57	17.58

In Fig. 7 we examine a variety of inversion strategies in an attempt to fit the data of site II/6. All models are constrained to include a resistive bottom layer of 1000 Ω m whose depth is a free parameter. From geological considerations it is reasonable to include such a layer because we expect a resistive basement beneath the Münchberg nappes. Judging from the MT data alone, its inclusion is less certain as the phases stay above 45° even at the longest periods of site WGL. While a resistive bottom layer may not be required to fit the data, it does not cause a contradiction, makes comparison of the different models easier, and provides some idea about the total conductance. Fig. 7(a) shows four different 1-D models. Model 1 comprises four layers with continuously increasing conductivity (plus the bottom layer of 1000 Ω m). Only the number of layers is determined *a priori* for the inversion, while resistivities and depths are free parameters. Model 2 is similar to Model 1, but with an additional thin layer of fixed thickness (250 m) and resistivity (0.01 Ω m). Model 3 is similar to Model 2, but comprises a stack of alternating thin conductive and resistive layers. Again, thicknesses (250 m) and resistivities (0.1 and 1000 Ω m, respectively) are fixed parameters. Model 4 is the result of a 1-D OCCAM inversion. Residuals of resistivity and phase over period and rms misfits are given in Fig. 7(b) for each model. The diagrams show that the rms misfits are mainly controlled by a few scattered data points with small error bars in the period range between 0.01 and 0.1 Hz (see Fig. 2 for the error bars). The residuals are calculated from the formulas

$$\mathrm{resid}(\ln \rho) = [\ln(\rho_{\mathrm{avg}}) - \ln(\rho_{\mathrm{mod}})]/\Delta\ln(\rho_{\mathrm{avg}}),$$

$$\mathrm{resid}(\Phi) = (\Phi_{\mathrm{avg}} - \Phi_{\mathrm{mod}})/\Delta\Phi_{\mathrm{avg}}.$$

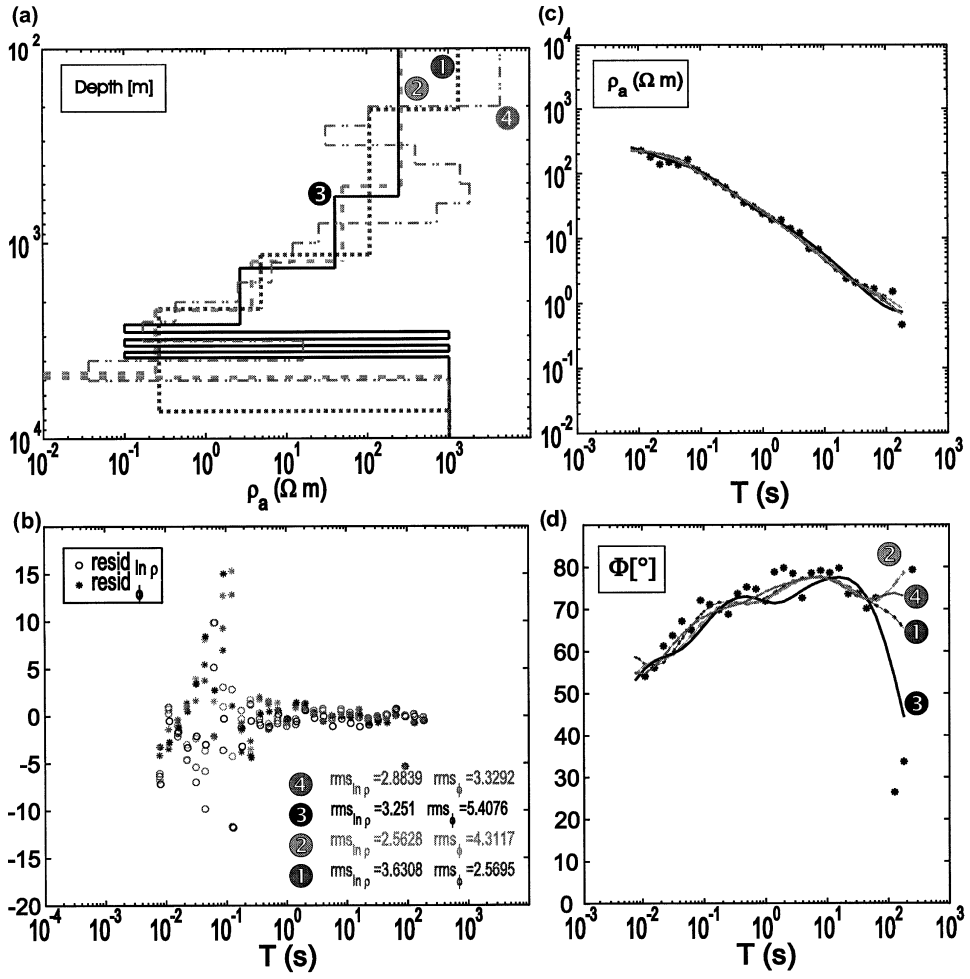

Figure 7. Comparison of various strategies to invert the averaged apparent resistivity and phase data of site II/6 (see text). (a) shows the models, (b) gives residuals (resid) and rms misfits, and (c) and (d) give model responses together with the field data. Obviously, only the general trend of continuously decreasing resistivities is common to models 1–3, while the geometry of the deepest conducting layer cannot be resolved. The bottom layer of model 1 indicates a total conductance of 19 000 S.

ρ_{avg}, $\Delta\rho_{avg}$ and Φ_{avg}, $\Delta\Phi_{avg}$ are the apparent resistivity and phase values, calculated from averaged impedances, and their respective absolute errors. ρ_{mod} and Φ_{mod} are 1-D modelling results. The rms misfits for n estimates of ρ_{avg} and Φ_{avg} are

$$\mathrm{rms}(\ln \rho) = [\Sigma_n \,\mathrm{resid}(\ln \rho)^2/n]^{1/2},$$

$$\mathrm{rms}(\Phi) = [\Sigma_n \,\mathrm{resid}(\Phi)^2/n]^{1/2}.$$

If the 1-D model responses are compared with the apparent resistivity and phase data in Figs 7(c) and (d), it becomes evident how alike these dissimilar models are in terms of model responses. The main common feature in the models is continuously increasing conductivity with depth. However, we cannot distinguish between a thin, very conductive layer, a stack of thin conductors, and a thick conductive layer.

To gain more structural information, which is obviously difficult from the magnetotelluric data alone, we can turn to the relevant section of the DEKORP 85-4N seismic reflection profile. The MüMa was investigated by reflection and refraction experiments. The most prominent seismic features are a highly reflective upper crust and a zone of very high velocities, rising from 5.6 km s^{-1} at a depth of 2 km to 7 km s^{-1} at about 5 km depth (Lang & Gebrande 1993). Behr *et al.* (1994) interpret the coherent reflectivity as due to the occurrence of mafic stratiform rocks in a metasedimentary assemblage deformed by low-angle thrusting. New geophysical data suggest that the high-velocity zone is not restricted to the MüMa formations but might extend as far as the SW margin of the Bohemian Massif (DEKORP & Orogenic Processes Research Groups 1999).

The depths of seismic reflectors imaged in migrated TWT-sections depend largely on the assumed near-surface seismic velocity structure, which is complicated and not very well known in the area. The 2-D velocity structure that was used to calculate the interface depths in the seismic section in Fig. 8 is a combination of a model estimated directly from rms velocities of the reflection data and a 1-D model derived from expanded spread seismic experiments for MVE90-CMP1 (Lang & Gebrande 1993) with significantly higher *P*-wave velocities. An individual application of these two different velocity models results in a depth variability of up to 1 km.

Fig. 8 shows the seismic reflection data in combination with the best-fitting four-layer models of sites I/3, II/6, and III/9. Each of the sites represents one station array; corresponding depths, resistivities and misfits are summarized in Fig. 6 and Table 2. Site III/9, at the centre of the MüMa, shows the highest resistivity for the top layer and the lowest resistivity for the bottom layer. This behaviour corresponds generally with the sandwich-type structure of the decreasing metamorphic grades of the MüMa rocks. Site II/6, located on Palaeozoic magmatic rocks at the boundary of the MüMa formations with the Bavarian facies, shows a more modest resistivity structure and, seen in conjunction with site III/9, rising interface depths. Site I/3, on the other hand, is situated on a NE–SW-trending band of outcropping Silurian and Cambrian metasedimentary rocks, which may explain the relatively high surface resistivities. At site I/3, the bottom layer with the highest conductivity is reached at about 3.5 km.

The band of the highest, most coherent reflectivity in Fig. 8 is found in the depth range between 2.5 and 5.5 km. Referring to the MVE90-CMP1 (Lang & Gebrande 1993) v_p velocity model for a petrological interpretation of this depth range, velocities of up to 7 km s^{-1} would indicate rocks of a high metamorphic or granulitic composition which are not usually associated with high conductivity. A more detailed discussion of the apparent discrepancy in the seismic velocities is beyond the scope of this paper.

UNDERSTANDING HIGH ELECTRICAL CONDUCTIVITY

Electrical resistivity is a property of rocks, as is, for example, their density. There is, however, a clear difference between the

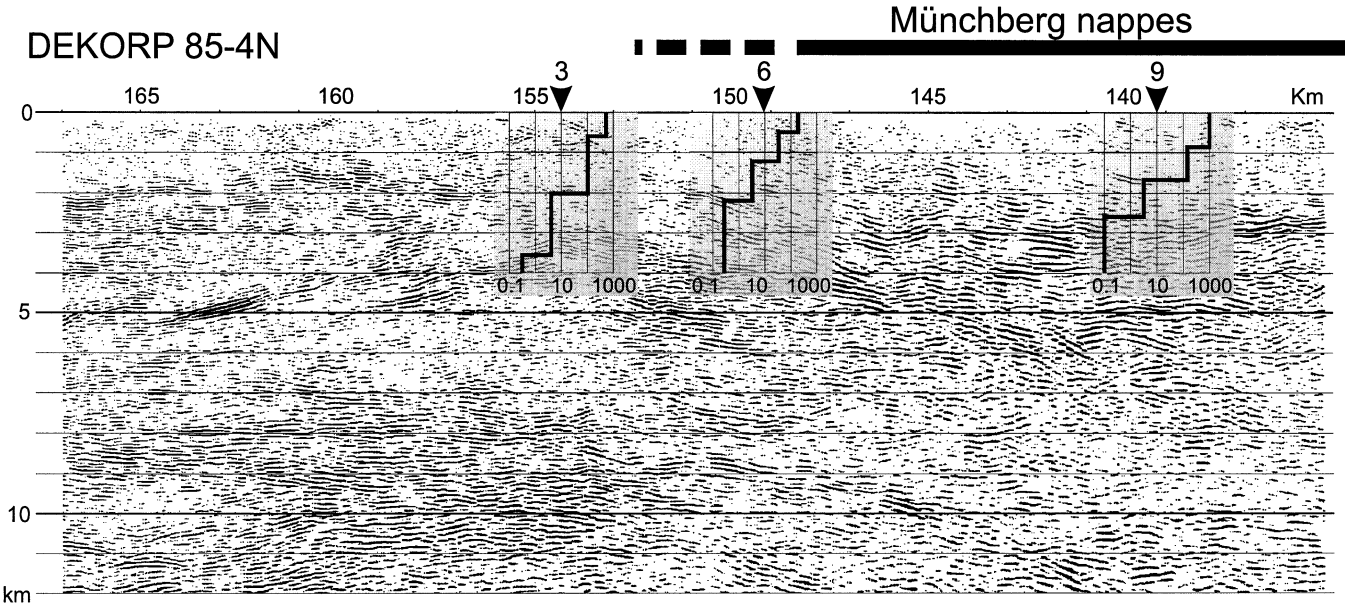

Figure 8. DEKORP 85-4N migrated seismic reflection line together with the best-fitting four-layer 1-D models of three MT sites. The depth to the best conducting layer at the MüMa sites II/6 and III/9 seems to correlate with the beginning of strong seismic reflectivity. The total overall conductance indicates that fluids alone cannot explain such high conductivity. Metallic conduction is a more consistent explanation, probably in the form of graphite, which was smeared-out along shear planes during transport of the MüMa nappes.

two properties. Density characterizes the type of rock, since it depends on the type of minerals of which the rock consists. The electrical resistivity, on the other hand, is usually not controlled by the major rock-building minerals but by the material in between these minerals: fluids, graphite, and ore minerals. It also depends on the interconnectivity of the materials. Intact rocks, in particular high grade metamorphic rocks, are usually highly resistive, with resistivities exceeding 10 000 Ω m.

These values remain the same under *in situ* conditions, demonstrated by the continuous measurements in the KTB Deep Drill hole which show resistivity values in excess of 100 000 Ω m at 9 km depth. Rock samples from the drill hole, mainly gneisses, contain even connate graphite and high-salinity fluids, which do not decrease the electrical resistivity. In the case of the KTB, interconnected, highly conductive phases exist only in shear zones in which the resistivity drops by seven orders of magnitude. High conductivity is caused both by high-salinity fluids and interconnected graphite, usually on slickensides (ELEKTB 1997).

The shearing has two functions with respect to the increase in conductivity. First, it creates space for the invasion of fluids. Second, the shearing process provides the tribochemical energy to form graphite from hydrocarbon-bearing fluids via the reaction $CO_2 + CH_4 \leftrightarrow 2H_2O + 2C$ (Kontny *et al.* 1997). The graphite is thereby actively deposited from this mixture of fluids by the shearing process. Further shearing causes smearing-out of formed graphite, and eventually interconnected films of graphite, as is the case in the slickensides. Graphite could also originate from the shearing of carbon layers in the sedimentary rock assemblages due to the transport of nappes; such 'internal' graphite enables the shearing but is not generated by the shearing.

In summary, we consider the dynamic processes associated with shear zones to be the primary source for high electrical conductivity, while the type of conductive material in shear zones is of secondary importance.

DISCUSSION AND CONCLUSIONS

With modern MT equipment and data processing tools it has become feasible to achieve reasonable results in electrically contaminated areas. Our data, collected at three station arrays along a profile across the Münchberg Massif, support this finding. The new data are of significantly better quality than those measured more than 15 years ago. Common to all sites are steeply decreasing apparent resistivity curves which indicate very high electrical conductivity with increasing depth.

1-D inversion of the apparent resistivity and phase curves results in layered models with continuously decreasing resistivities. The bottom layers yield resistivities below 1 Ω m at approximately 2.5–3.5 km depth at all sites. The 1-D models can explain most aspects of the apparent resistivity and phase data at shorter periods (<100 s). The relatively sparse site spacing hinders construction of a more detailed structural electrical image of the MüMa, although there is some evidence in the vertical magnetic field transfer functions for a lateral change in conductivity between station arrays II and III. From the MT data alone it is not possible to decide whether the conductivity at depth is caused by a thin, very conductive layer, a stack of thin conductors, or an extended, thick conductive layer. However, at least for the sites close to or on the MüMa, the depth of the best conducting layer coincides with the beginning of strong seismic reflectivity (DEKORP85 4N) at a depth between 2.5 and 5.5 km. From the MVE90-CMP1 v_p velocity model, this depth range is associated with rocks of a high metamorphic or granulitic composition.

The metamorphic rock complex of the MüMa is an allochthonous part of the Variscan basement in NE Bavaria which has been identified as a crystalline nappe for a number of geological and petrological reasons that are beyond the scope of this paper. If the MüMa is a crystalline nappe, it must have been pushed to its present position by a tectonic process several hundred million years ago. What traces are left behind from this process? What are the geoscientific methods suitable to detect such traces?

Our magnetotelluric experiment discovered zones of high electrical conductivity in the uppermost crust beneath or within the highly resistive metamorphic rocks of the MüMa, not deeper than 1–3 km. The lower boundary of the deepest high-conductivity layer is not well resolved (see Table 2). Periods longer than 100 s are required to resolve the total conductance. However, it is plausible to conclude that the conductance of the deepest conducting layer of model 1 in Fig. 7 represents a lower limit of the true conductance. The conductance of this layer exceeds 19 000 S! If we take this value, assume high-salinity fluids of $\rho_0 = 1/100$ Ω m and a porosity (F) of 10 per cent, then, according to Archie's law ($\rho_a = \rho_0 F^{-2}$), a conductance of 19 000 S would require a layer 19 km thick. This thickness contradicts our modelling results in Fig. 7. More realistic values ($\rho_0 = 1/10$ Ω m, 1 per cent porosity) would result in an even thicker layer (1900 km!) of high conductivity. This result means that saline fluids alone cannot explain our observations. There is no realistic explanation other than to assume metallic conduction, perhaps in combination with electrolytic conduction. The electrical conductivity of graphite is several orders of magnitude higher than that of saline fluids, and, if intensively interconnected, requires a layer thickness of less than 1 km. The lesson we learned from the KTB study (ELEKTB 1997) was that connate graphite in the gneisses does not increase the electrical conductivity at all, because it is not interconnected. It is the graphite formed on shear planes that is well interconnected and thus highly conductive.

Graphite is a very effective lubricating element. If the results from the KTB can be transferred to the MüMa, then the shear planes and the graphite on them were created in the deep Variscan crust. Thus, the movement along shear zones seems to be responsible for this high-conductivity anomaly; the mere existence of the conducting material is insufficient. Materials (like graphite) which increase the electrical conductivity may also increase the mobility, which would imply a common origin of conductivity and mobility.

Furthermore, the 1-D, layered character of the conductivity anomaly could hint at a new, more complicated, two-phase scenario for the accretion of the MüMa nappes: the Randamphibolite represents the basal part of the crystalline thrust sheets which were accreted towards the west and later overthrust towards the northwest onto the sediments of the Bavarian facies as a complex of thrust sheets, from the Randamphibolite as its footwall to the Hangend Serie as hanging wall. There are no indications for metamorphic events after 365 Ma and temperatures must have been below 300 °C since then. This means that the lower Carboniferous sediments

could not have been deposited at that time. Therefore, there must have been a second, compressional tectonic event after the lower Carboniferous sedimentation, with an accretion of the (meta-)sedimentary thrust sheets and their final emplacement towards the northwest. The crystalline thrust sheets were transported passively as an entire complex. Such a two-phase tectonic environment could have left two major shear planes which we might have detected as electrical conductors. In that respect, magnetotelluric measurements can give us insight today into dynamic processes of the Earth's history.

ACKNOWLEDGMENTS

We would like to thank Uli Kalberkamp, Achim Helm, and Markus Himmerich for their help during the field work. We are grateful for the very helpful comments of two anonymous referees.

REFERENCES

Bahr, K., 1988. Interpretation of the magnetotelluric impedance tensor: regional induction local telluric distortion, *J. Geophys.,* **62,** 119–127.

Behr, H.-J. & DEKORP Research Group (B), 1994. Crustal structure of the Saxothuringian Zone: Results of the deep seismic profile MVE-90 (East), *Z. geol. Wiss.,* **22,** 647–769.

Börner, R.-U., 1995. Die Leitfähigkeitsverteilung der Erdkruste zwischen Frankenwald und Harz—abgeleitet aus der Inversion magnetotellurischer Messungen, *PhD thesis,* Technische Universität Bergakademie Freiberg.

Dawes, G.J.K., 1990. Feasibility study for a transputer-based upgrade of the Short-Period Automatic Magnetotelluric S.P.A.M.-system, NERC report F3/G6/S43, University of Edinburgh.

DeGroot-Hedlin, C. & Constable, S., 1990. Occam's inversion to generate smooth two dimensional models from magnetotelluric data, *Geophysics,* **55,** 1613–1624.

DEKORP & Orogenic Processes Working Groups, 1999. Structure of the Saxonian Granulites—geological and geophysical constraints on the exhumation of HP/HT rocks in the mid-European Variscan belt, *Tectonics,* in press.

Egbert, G.D., 1997. Robust multiple-station magnetotelluric data processing, *Geophys. J. Int.,* **130,** 475–496.

Egbert, G.D. & Booker, J.R., 1986. Robust estimation of geomagnetic transfer functions, *Geophys. J. R. astr. Soc.,* **87,** 173–194.

ELEKTB Group, 1997. KTB and the electrical conductivity of the crust, *J. geophys. Res.,* **102** (B8), 18 289–18 305.

Franke, W., 1984. Variszischer Deckenbau im Raume der Münchberger Gneismasse- abgeleitet aus der Fazies, Deformation und Metamorphose im umgebenden Paläoziokum, *Geotekt. Forsch.,* Vol. 68, Nägele & Obermüller, Stuttgart.

Franke, W., Kreuzer, H., Okrusch, M., Schüssler, U. & Seidel, E., 1995. Saxothuringian Basin: exotic metamorphic nappes: stratigraphy, structure, and igneous activity, in *Pre-Permian Geology of Central and Western Europe,* pp. 277–294, eds Dallmeyer, R.D., Franke, W. & Weber, K., Springer-Verlag, Heidelberg.

Geotools, 1997. *Geotools MT Users's Guide,* Geotools Corp., Austin, TX.

Groom, R.W. & Bailey, R.C., 1989. Decomposition of magnetotelluric impedance tensors in the presence of local three-dimensional galvanic distortion, *J. geophys Res.,* **94** (B2), 1913–1925.

Gürtler, J. & Schwarz, G., 1994. Interpretation of a MT Profile from the Frankenwald to the Harz Mountains, *Potokoll Kolloquium Elektromagnetische Tiefenforschung,* eds Bahr, K. & Junge, A., Hoechst (in German).

Haak, V., Blümecke, Th., Fischer, G., Schnegg, P. & Rath, V., 1985. Electrical conductivity studies, Oberpfalz, in *Abstract 2nd Int. Symp. on Observation of the Continental Crust through Drilling,* p. 55, Seeheim, Germany.

Kontny, A., Friedrich, G., Behr, H.J., de Wall, H., Horn, E.E., Möller, P. & Zulauf, G., 1997. Formation of ore minerals in metamorphic rocks of the German continental deep drilling site (KTB), *J. geophys. Res.,* **102** (B8), 18 323–18 336.

Lang, M. & Gebrande, H., 1993. Seismische Geschwindigkeiten in der Münchberger Gneismasse, *Z. geol. Wiss.,* **21,** 172–177.

Larsen, J.C., Mackie, R.L., Manzella, A., Fiordelisi, A. & Rieven, S., 1996. Robust smooth magnetotelluric transfer functions, *Geophys. J. Int.,* **124,** 801–819.

Müller-Sohnius, D., Von-Drach, V., Horn, P. & Koehler, H., 1987. Altersbestimmungen an der Münchberger Gneismasse, Nordost-Bayern, *Neues Jahrbuch fuer Mineralogie,* Abhandlungen, E. Schweizerbart'sche Verlagsbuchhandlung, Stuttgart, **156 (2),** 175–206.

O'Brien, P., 1996. Eclogites and related rocks in the Münchberg Massif.–6, *EMPG Tagung, Exkursionsführer 13.4.96,* University of Bayreuth.

Pflug, H.D. & Reitz, E., 1987. Palynology in metamorphic rocks: indication of early land plants, *Naturwissenschaften,* **74,** 386–387.

Ritter, O., Junge, A. & Dawes, G.J.K., 1998. New equipment and processing for magnetotelluric remote reference observations, *Geophys. J. Int.,* **132,** 535–548.

Schäfer, F., 1997. Krustenbilanzierung eines variscischen Retrokeils im Saxothuringikum, *PhD thesis,* Freie Universität Berlin.

Stosch, H.G. & Lugmair, G.W., 1990. Geochemistry and evolution of MORB-type eclogites from the Muenchberg Massif, southern Germany, *Earth planet. Sci. Lett.,* **99,** 230–249.

Weber, K. & Behr, H.J., 1983. Geodynamic interpretation of Mid-European Variscides; case studies in the Variscan Belt of Europe and the Damara Belt in Namibia, in *Intracontinental Fold Belts,* pp. 427–469, eds Martin, H. & Eder, F.W., Springer Verlag, Heidelberg.